Langmuir

Article

pubs.acs.org/Langmuir

Stabilization of Insulin by Adsorption on a Hydrophobic Silane Self-Assembled Monolayer

Sergio Mauri,[†,‡] Martin Volk,[†] Stephen Byard,[§] Harald Berchtold,[∥] and Heike Arnolds*[,†]

[†]Department of Chemistry, Surface Science Research Centre, University of Liverpool, Oxford Road, Liverpool L69 3BZ, U.K.

[‡]Molecular Spectroscopy Group, Max Planck Institute for Polymer Research, Ackermannweg 10, 55128 Mainz, Germany

[§]Covance Inc., Willowburn Avenue, Alnwick NE66 2JH, U.K.

[∥]Sanofi-Aventis Deutschland GmbH, R&D LGCR/Analytical Sciences FF, Industriepark Hoechst, D-65926 Frankfurt am Main, Germany

Supporting Information

ABSTRACT: The interaction between many proteins and hydrophobic functionalized surfaces is known to induce β-sheet and amyloid fibril formation. In particular, insulin has served as a model peptide to understand such fibrillation, but the early stages of insulin misfolding and the influence of the surface have not been followed in detail under the acidic conditions relevant to the synthesis and purification of insulin. Here we compare the adsorption of human insulin on a hydrophobic ($-CH_3$-terminated) silane self-assembled monolayer to a hydrophilic ($-NH_3^+$-terminated) layer. We monitor the secondary structure of insulin with Fourier transform infrared attenuated total reflection and side-chain orientation with sum frequency spectroscopy. Adsorbed insulin retains a close-to-native secondary structure on both hydrophobic and hydrophilic surfaces for extended periods at room temperature and converts to a β-sheet-rich structure only at elevated temperature. We propose that the known acid stabilization of human insulin and the protection of the aggregation-prone hydrophobic domains on the insulin monomer by adsorption on the hydrophobic surface work together to inhibit fibril formation at room temperature.

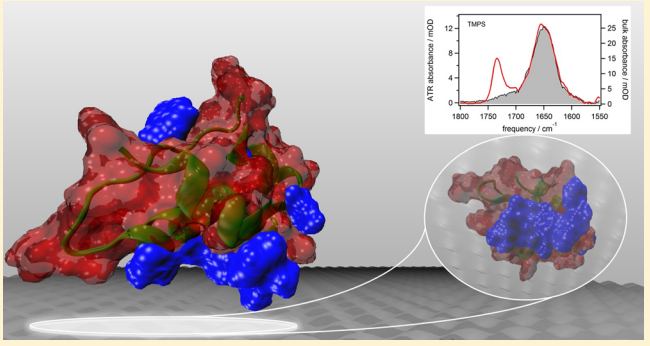

INTRODUCTION

The formation of insoluble amyloid fibrils is responsible for the deterioration of valuable therapeutic proteins during production, storage, and injection and also lies at the origin of several degenerative diseases such as Alzheimer's and type II diabetes.[1,2] In these areas, insulin has played a pivotal role as model system in understanding fibril formation and inhibition.[3−5] Insulin is a small, globular protein of 51 amino acids arranged in two chains, with a mainly α-helical structure stabilized by three disulfide bonds (Figure 1). In solution, monomers can form dimers to shield a hydrophobic domain on the monomer surface from the solvent. At high concentrations and particularly in the presence of zinc ions, dimers can further self-assemble to hexamers, which protect insulin from fibrillation in vivo. The insulin monomer is the physiologically active species and is also the key species in forming amyloids in vitro. In solution at low pH, partially unfolded monomers have been identified as being on the pathway to fibril growth, and their structure has been unravelled.[6,7]

The acceleration of amyloid formation by interfaces is similarly attributed to the stabilization of partially unfolded adsorbed insulin monomers, which go on to form different fibril morphologies from the bulk.[8−10] Most detailed structural

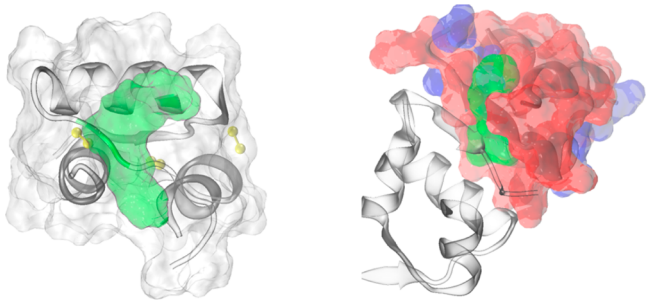

Figure 1. Sketch of the insulin monomer (left—protein data bank ID 2JV1[17]) and insulin dimer (right—protein data bank ID 4INS[18]). The insulin B chain (long helix with four turns) is connected via disulfide bonds (yellow) to the A chain (two helices). The hydrophobic part of the dimer interface is marked in green, other hydrophobic parts are colored blue, and the hydrophilic-solvent-accessible region is marked in red. Structures are visualized using VMD.[19]

Received: April 22, 2015
Revised: June 23, 2015
Published: July 25, 2015

DOI: 10.1021/acs.langmuir.5b01477
Langmuir 2015, 31, 8892−8900

studies have been carried out at physiological pH, from which the following picture of insulin adsorption emerges. Insulin monomers often form a close-packed monolayer at hydrophobic interfaces, where they lose α-helical structure and gain random-coil or β-sheet structure.[10−14] Conformational changes in adsorbed insulin appear to allow further binding from solution, such that preadsorbed peptides with a β-sheet structure were found to accelerate surface-induced insulin fibrillation.[15,16]

Here we concentrate on acidic environments encountered during the synthesis and purification of insulin. Under these conditions, insulin predominantly exists as monomers in solution, which allows us to focus our attention on the monomer's interaction with surfaces. Prior work at low pH has investigated only the kinetics of fibril formation at hydrophobic interfaces[8,9] or developed soft surface coatings such as polyelectrolyte multilayers, where the protein penetrates the multilayer deeply and remains stable at low pH and elevated temperature.[20] There are no comparable studies of adsorption on the hard surfaces typically encountered during insulin production or storage. The little attention bestowed upon such surface characterization in insulin aggregation studies at low pH and the scarcity of structural information for submonolayer to low multilayer insulin coverage leaves open questions: what is the structure of adsorbed insulin monomers at low pH, and what is the nature of intermediates on the path to fibril formation?

In this study, we use well-characterized hydrophobic and charged hydrophilic silane self-assembled monolayers (SAMs) formed on silicon surfaces and employ a combination of electronic and vibrational spectroscopies to elucidate the nature of the surface−insulin interaction. We compare the adsorption of insulin on a hydrophobic surface to adsorption on a charged hydrophilic surface, which is known to keep porcine insulin physiologically active.[21] To understand insulin adsorption, we quantify the adsorbed amount by X-ray photoelectron spectroscopy (XPS), quartz-crystal microbalance with dissipation (QCM-D), and Fourier transform infrared with attenuated total reflection (FTIR-ATR), we analyze the silane SAM and insulin side-chain orientation by sum frequency spectroscopy (SFS), and finally we use FTIR-ATR to investigate the secondary structure of monolayer insulin at room temperature and later unfolding and multilayer growth at elevated temperature.

Surprisingly, we find that the native structure of insulin monomers is maintained upon adsorption at room temperature and that only incubation at high temperature creates adsorbed insulin with a significant β-sheet content.

EXPERIMENTAL SECTION

Sample Preparation. Si wafers for SFS and the Si ATR crystal were cleaned using piranha solution (70% H_2SO_4, 30% H_2O_2 solution (35% in water)) for 10 min at room temperature in a sonication bath. QCM crystals were cleaned using UV ozone and only briefly dipped into cold piranha solution (3 min at room temperature). After cleaning, all samples were thoroughly rinsed with copious amounts of ultrapure water (18.2 MΩ) and dried under a flow of argon. All glassware was cleaned in piranha solution at 70 °C for 1 h, rinsed several times with ultrapure water and ethanol, dried under a stream of dry air, and finally rinsed with toluene. Trimethoxypropylsilane (TMPS, $CH_3(CH_2)_2Si(OCH_3)_3$) and 3-aminopropyltrimethoxysilane (APTMS, $H_2N(CH_2)_3Si(OCH_3)_3$) solutions were prepared in toluene at concentrations of 5 mM and 0.5 mM, respectively. By using anhydrous solvents and low concentrations, we avoided the well-known polymerization reaction and multilayer formation of APTMS.[22] Silicon wafers were left in silane solution for 24 h at room temperature, sonicated in toluene to remove potential multilayers, and rinsed with copious amounts of ultrapure water. Finally, substrates were dried under a flow of argon. Human insulin with 0.3% Zn by weight was kindly provided by Sanofi-Aventis Deutschland GmbH and used at a concentration of 0.44 mg/mL (75 μM). We prepared citrate−phosphate buffers at an ionic strength of 0.05 M at pH 2.7 for QCM-D and SFS analyses and deuterated buffer at pD 2.7 (measured pH* 2.3) for FTIR. Citrate has the benefit of binding zinc ions and thus countering the oligomerizing effect of zinc on insulin.[23] Functionalized silicon wafers used in the SFS experiments were left in contact with insulin solutions at pH 2.7 for 1 h, rinsed with ultrapure water afterward, and dried under a flow of argon.

Spectroscopy. To monitor the amount of adsorbed protein under flow, we used QCM-D on a Q-sense E4 (Biolin Scientific) with silicon-coated quartz sensors. XPS spectra of the sensors were recorded on a PSP Vacuum Technology analyzer at 0.5 eV resolution for survey spectra and 0.025 eV resolution for the analysis of binding-energy shifts. The $2p_{1/2}$ level of argon embedded in the silicon crystal was used as an internal energy standard with an energy of 241.2 eV.[24] FTIR measurements were performed using a Bruker IFS 66v/S spectrometer. Each spectrum was averaged over 500 scans at 1 cm^{-1} resolution. We used an ATR setup from Pike Technologies fitted with a silicon crystal (80 × 10 × 4 mm^3, 45°, 10 reflections). FTIR-ATR spectra of insulin recorded in D_2O show a broad peak around 1647 cm^{-1} and no amide II band around 1550 cm^{-1}, indicating complete H/D exchange.[25] Sum frequency spectroscopy (SFS) is a second-order nonlinear optical technique which intrinsically provides surface sensitivity and high spectral resolution and represents a coherent combination of infrared absorption and a Raman anti-Stokes transition. SFS was recorded on Si(100) wafers with a 1 kHz amplified Ti/sapphire laser system from Coherent Inc. The laser output was used both to generate a 7 cm^{-1} narrow-band 800 nm beam with an etalon and to pump a commercial OPA (OPerA Solo from Coherent Inc.) for tunable broadband IR light generation. Spectra in the ppp polarization combination were collected by a spectrograph equipped with an iCCD camera from Andor with an 800 fs time-delayed etalon pulse to suppress the nonresonant response of the silicon substrate. The intensity in SFG spectra can then be described as $I \approx |\chi_{res}|^2$, where $\chi_{res} = \sum_i((A_i)/(\omega_i - \omega + i\Gamma_i))$ with A_i, ω_i, Γ_i being the amplitude, frequency, and width of the Ith resonance and ω being the frequency of the IR pulse. In the analysis of the methyl group orientation we used the Lorentzian peak height $(A/\Gamma)^2$.[26] Further details can be found in the Supporting Information.

RESULTS

The advantage of studying insulin adsorption at acidic pH is that insulin exists predominantly as monomers and the monomer has been shown to be the only species that adsorbs to surfaces and subsequently denatures to form amyloid fibrils.[10,11] Insulin self-associates in solution to form dimers and hexamers, with the monomer favored at low concentration, in the absence of zinc ions, and at low pH.[10,27,28] The monomer has a tendency to segregate to hydrophobic interfaces, as we recently demonstrated for the air/water interface by SFS.[29] At our relatively low concentration of insulin (<0.5 mg/mL) and neutral pH, human insulin with zinc consists of 90% monomers and 10% dimers.[10] With decreasing pH, this ratio will shift even further toward the monomer.[30] At our chosen pH 2.7, insulin carries a positive charge of $z = 4.5$.[31] The Debye length of our citrate-phosphate buffer is relatively long at 1.4 nm such that repulsive interactions between insulin molecules will disfavor rapid multilayer growth and allow us to look at conformational changes in the insulin monolayer.

Quantification of Insulin Adsorption. We employ three experimental methods (QCM-D, XPS, and FTIR-ATR) to investigate the adsorption of insulin quantitatively. QCM-D

DOI: 10.1021/acs.langmuir.5b01477
Langmuir 2015, 31, 8892−8900

measures the mass of adsorbed insulin plus its hydration layer as a frequency shift of the shear vibration of a Si-coated quartz crystal. Since the viscosity and density of the liquid flowing across the quartz crystal also influence the frequency, we used a flow sequence of ultrapure water, buffer, insulin in buffer, buffer, ultrapure water to determine the pure adsorption-induced frequency shift. After switching from buffer to buffer + insulin, the frequency stabilized within 5 min, and no further changes were seen in the following 20 min of flowing insulin solution (Figure S4 in the Supporting Information). Insulin adsorption renders the previously hydrophobic TMPS-terminated surface hydrophilic, and quartz crystals removed at the end of the experiment possess a very low water contact angle. XPS recorded on the same crystals after QCM-D experiments determines the dried protein mass from the atomic fraction of nitrogen in the adsorbed protein in relation to the atomic fraction of nitrogen on the surface. In comparison, FTIR-ATR determines the concentration of insulin in the near surface layer of a polycrystalline silicon crystal in contact with an insulin solution from the absorbance in the amide I region. The results obtained with all three methods are summarized in Table 1, and

Table 1. Comparison of Three Experimental Methods (QCM-D, XPS, ATR-FTIR) to Determine Insulin Coverage on APTMS- and TMPS-Functionalized Surfaces at pH 2.7 after Incubation for 25−30 Minutes

insulin coverage/mg m^{-2}	QCM-D	XPS	ATR-FTIR[a]
APTMS	0.10	0.09	1.22
TMPS	1.05	0.67	1.35

[a]Values include the physisorbed layer.

further details can be found in the Supporting Information (SI). It can be seen that the hydrophobic TMPS surface has a coverage that is close to the theoretical insulin monolayer coverage of 1.1 mg/m^2, based on a rectangular close-packed layer.[23] The XPS value is about 36% lower than the QCM-D value, as expected from the loss of the hydration layer.[32] The hydrophilic APTMS-functionalized surface shows a much reduced insulin coverage, only just outside the detection limit of QCM-D. This is probably caused by the mutual repulsion between positively charged insulin and the positively charged surface at this pH. As Table 1 shows, the FTIR-derived coverages recorded in the presence of insulin solution are higher than the coverages determined by QCM-D or XPS. The difference is due to the formation of a physisorbed insulin layer, which is removed from the QCM-D crystal by rinsing with buffer and water. The effect is particularly pronounced on the positively charged hydrophilic surface, which prevents the formation of a strongly adsorbed layer of the equally positively charged insulin.

All three methods confirm that only a monolayer of insulin adsorbs at room temperature and pH 2.7 after incubation for half an hour. This compares well with literature values for adsorption at physiological pH 7.4 at hydrophobic surfaces such as Teflon,[12,13] polystyrene,[14] and methyl-terminated alkanes,[11,15] which are all in the 1−3 mg/m^2 range. There are no comparable quantitative data for these rigid surfaces at acidic pH. Experiments at polyacrylic brushes[33] and charged lipid layers[8] at pH 2 or lower detected much higher adsorbed masses of between 4 and 20 mg/m^2.

SAM and Protein Side-Chain Orientation. Sum-frequency spectra of siloxane films grown on Si(100) wafers are shown in Figure 2. The TMPS film possesses a well-defined sum frequency spectrum, which consists entirely of three CH_3-

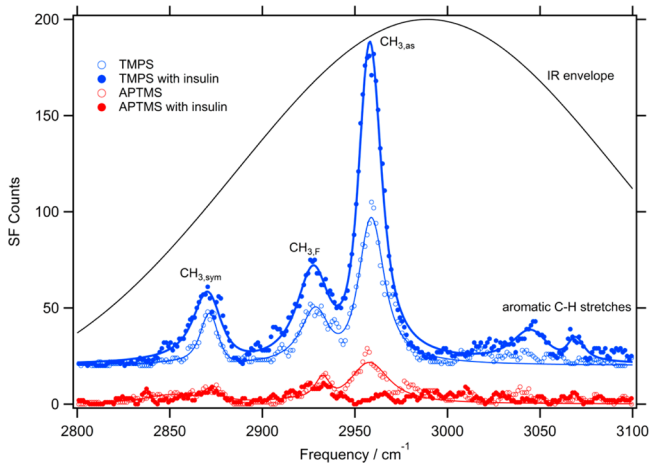

Figure 2. Sum frequency spectra of dried hydrophobic and hydrophilic silane layers grown on Si(100) before (open symbols) and after (filled symbols) insulin adsorption at pH 2.7. The envelope of the infrared pulse is shown as a thin black line.

related vibrational modes: the symmetric stretch at 2872 cm^{-1}, the asymmetric stretch at 2959 cm^{-1} and the Fermi resonance between the symmetric stretch and the overtone of the CH_3 bend at 2929 cm^{-1}. These frequencies are close to those found for C_{18} siloxanes on fused silica or glass.[34,35] The approximate center of inversion between the two CH_2 groups in an all-trans propyl chain prevents the generation of a sum frequency signal from these groups.[26,36,37] The lack of any CH_2-related signal in SFS thus shows the formation of a well-ordered film.

The APTMS film produces a similar-looking but much weaker SFS spectrum, which we propose to be due to CH_3 vibrations from unreacted methoxy groups.[22] This assignment is confirmed by XPS, where around 10% of the C 1s signal can be attributed to unreacted methoxy at a binding energy of 286.8 eV. The phase of the sum frequency light emitted by the CH_3 resonances with respect to the silicon nonresonant background is the same for TMPS and APTMS (spectra not shown), which implies that both methyl groups have the same general orientation,[38] that is, pointing up from the silicon surface. This is also supported by XPS N 1s spectra shown in the Supporting Information, which are composed of an NH_3^+ peak at 401.9 eV binding energy[39] and a peak at 400.2 eV typically assigned to NH_2 (Figure S2). Given the nonaqueous method of surface preparation, the most likely mechanism for protonation is by hydrogen bonding to surface silanol groups. The 4:3 ratio of NH_3^+ to NH_2 shows that about half of the APTMS chains are lying flat on the surface, compatible with unreacted methoxy groups pointing upward.[40]

We can deduce the angle of the CH_3 symmetry axis with respect to the surface normal from the intensity ratio between asymmetric and symmetric peaks:[26,36,41]

$$R = \frac{I_{asym}}{I_{sym} + I_F}$$

To relate this ratio to a methyl tilt angle, we calculate hyperpolarizability values for methyl and methylene groups using the bond additivity model.[42,43] We account for the reduction of the symmetric sum frequency signal by intensity

DOI: 10.1021/acs.langmuir.5b01477
Langmuir 2015, 31, 8892−8900

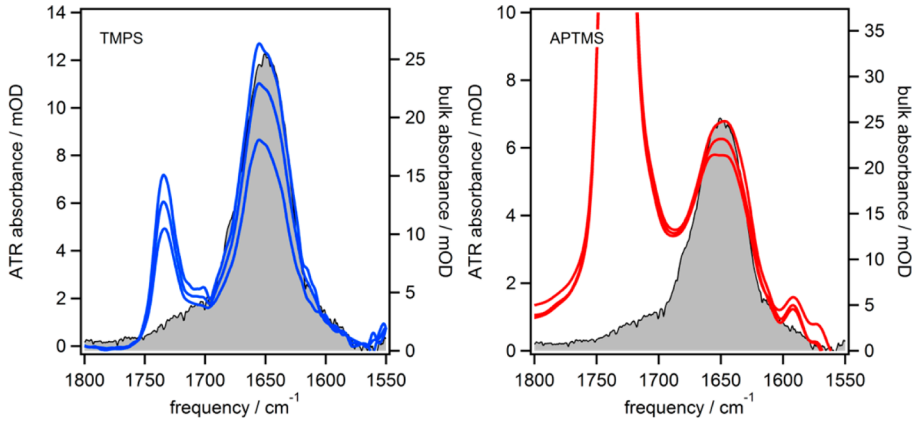

Figure 3. ATR-FTIR spectra of TMPS- (blue) and APTMS-terminated silicon surfaces (red) during insulin incubation in buffered D_2O at pD 2.7 are compared to bulk insulin spectra (shaded gray, right axis). Spectra took 30 min to record, and the pure buffer spectra have been subtracted. The lowest spectrum was recorded during the first 30 min of adsorption, the middle one between 1 and 1 h 30 min, and the highest one between 2 and 2 h 30 min.

splitting between the symmetric CH_3 stretch and the Fermi resonance and use the recorded FTIR spectra to deduce the degree of intensity sharing.[26] Details of the calculation can be found in the SI. We obtain R = 0.89 from the experimental TMPS/Si(100) spectrum, which corresponds to a tilt angle of 31° for the methyl group and an angle of ~6° for the propyl backbone, slightly lower than the backbone tilt angle of around 15° deduced by SFS for a C_{18} silane chain on glass.[44] For the hydrophilic APTMS/Si(100), we obtain a very similar tilt angle of 34° for the CH_3 of the methoxy group.

Insulin adsorption leads to clear changes in the sum frequency spectra of both layers. On the hydrophobic surface, the asymmetric CH_3 peak grows in relationship to the two symmetric peaks such that the asymmetric to symmetric ratio increases from 0.89 to 1.58. The width of the two symmetric peaks increases significantly, while that of the asymmetric peak remains the same, suggesting that this spectrum could have small contributions from nearby CH_2 groups, although they are not distinct enough to be fit separately. In addition, two clear peaks in the aromatic C−H stretching region appear at 3045 and 3068 cm^{-1}.

This change in the asymmetric to symmetric intensity ratio could be due to a hydrophobic interaction between insulin and TMPS which increases the tilt angle of the surface methyl groups. It could also stem from a net orientation of insulin side chains on the hydrophobic surface, as observed for amino acids[45] and polypeptides and proteins.[46,47] If the change was purely due to a hydrophobic effect, then the increase in the asymmetric/symmetric peak ratio to 1.58 would correspond to a 5° increase in the tilt angle of the methyl group. This is comparable to other hydrophobic interactions measured by SFS, for example, the 3.3° increase in the CH_3 tilt angle of octadecanethiol on Au(111) when the solvent was changed from distilled water to a hydrophobic bacterium.[48] However, the appearance of aromatic C−H peaks from phenylalanine and tyrosine side chains clearly shows that insulin adsorbs in an ordered fashion on the hydrophobic surface and that a pure hydrophobic effect is unlikely to be the sole cause of the observed change. If insulin adsorbs with the hydrophobic dimer interface toward the hydrophobic surface (the most likely orientation; see the Discussion section), then its 28 methyl groups are oriented in such a way as to make a net contribution of 10 CH_3 groups to a sum frequency spectrum at a tilt angle of 65°, while its 54 methylene groups make a net contribution of only 7 CH_2 groups at a tilt angle of 32° (Supporting Information). In this orientation, the net intensity of the CH_3 asymmetric stretch would be several times larger than the net CH_2 signal, which can qualitatively explain the observed changes in the aliphatic C−H stretching region. It is difficult to extract further information without isotopic substitution, though, because the total spectrum contains contributions from both insulin and TMPS.

On APTMS, on the other hand, insulin adsorption leads to an almost complete disappearance of the asymmetric CH_3 stretch, so either the residual methoxy groups tilt upward or insulin adsorbs in such a way as to cancel this signal. The overall small signal indicates there is no net orientation of side chains.

Protein Structure. The amide I band provides a sensitive indicator of protein secondary structure, with α-helical structures in D_2O generating resonances in the range of 1630−1650 cm^{-1} and β-sheets generating a main peak at around 1615−1638 cm^{-1}, with a minor peak in the range of 1672−1694 cm^{-1}.[49] Native insulin in solution is mostly α-helical with a peak at 1649 cm^{-1}. Upon heating and shaking, a 75 μM solution forms β-sheets with a main peak at 1623 cm^{-1} and a shoulder at 1697 cm^{-1} (Supporting Information). The expectation from the literature for the secondary structure of adsorbed insulin is a decrease in α-helical content and an increase in β-sheets or random coil content. This was deduced from UV circular dichroism spectra on Teflon and polystyrene beads at pH 7.4,[10,13,14] while an FTIR-ATR study of insulin adsorbed on a phenyldimethyl-functionalized silicon crystal interpreted a peak at 1708 cm^{-1} as the appearance of intermolecular β-sheets.[15] In Figure 3, we show the amide I region during insulin adsorption on TMPS- and APTMS-modified silicon at pD 2.7 in buffered D_2O, after pure buffer spectrum subtraction. Insulin in the bulk solution contributes at most 1.2 mOD to the peak signal (Supporting Information), which thus dominantly shows the adsorbed layer. The narrow peak at 1734 cm^{-1} is due to the C═O stretch in the carboxylate groups of citric acid and indicates an increased concentration of citric acid in the near surface layer when insulin adsorbs. At pD 2.7, some of the carboxyl groups are deprotonated and can bind to several hydrogen bond donors in insulin, specifically amine or hydroxyl groups, as observed in

DOI: 10.1021/acs.langmuir.5b01477
Langmuir 2015, 31, 8892−8900

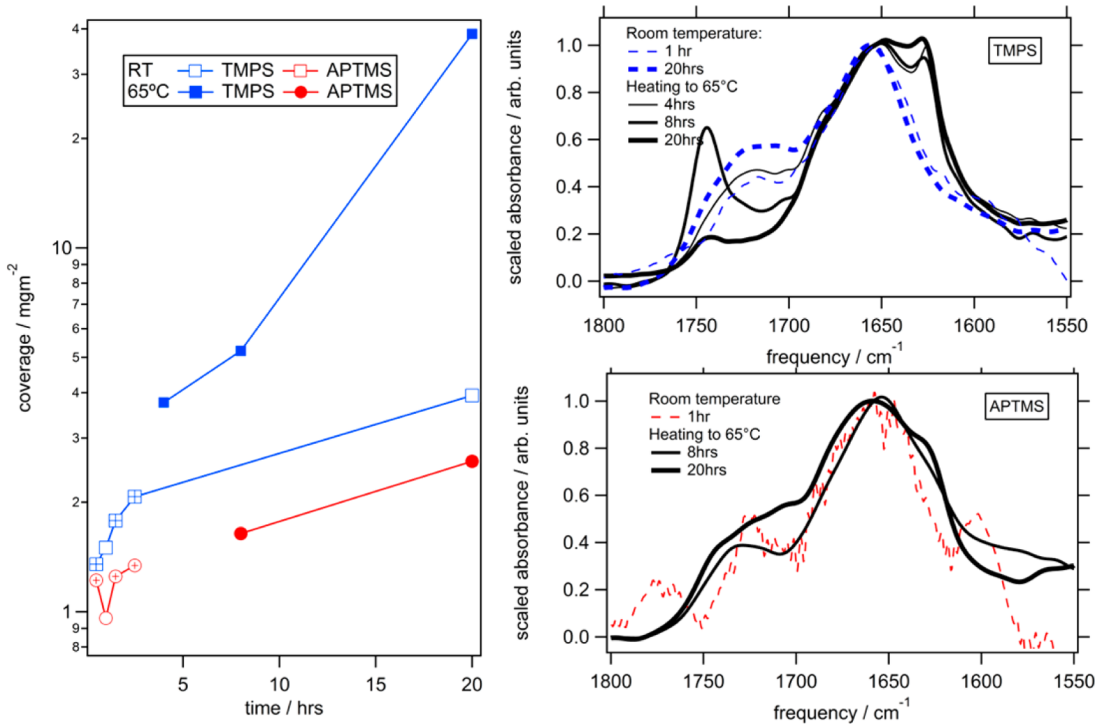

Figure 4. Insulin adsorption at room temperature and at elevated temperature in buffered D_2O at pD 2.7 determined by means of ATR-FTIR. Left: Coverage as a function of adsorption time at room temperature (open symbols for dried layers measured ex situ, crossed symbols for wet layers measured in situ) and at 65 °C (closed symbols for dried TMPS (blue) and APTMS (red) layers). Lines are used to guide the eye. Right: Scaled ATR-FTIR spectra of dried layers to show the change in the amide I band shape for TMPS- (top) and APTMS-terminated surfaces (bottom).

the solution spectra of bovine insulin in acetic acid.[25] The much more intense C═O peak on the APTMS-functionalized surface arises from citrate binding to surface amine groups, which are also hydrogen donors.

The amide I peak of insulin itself occurs at 1650 cm^{-1}. As the overlaid solution spectra show, the shape of the amide I peak of adsorbed insulin is extremely similar to that of native insulin in solution and does not change appreciably over the course of 3 h at room temperature. A 1 cm^{-1} shift toward higher frequencies can be seen for the TMPS spectra, which could indicate a small increase in the random coil content or alternatively a small amount of desolvation, while the width of the amide I peak on APTMS increases by 10%, which could indicate a small amount of disorder. Overall, however, under these conditions, the secondary structure of insulin is hardly affected by adsorption, and both hydrophobic and hydrophilic surfaces are as protein-friendly as polyelectrolyte brushes.[20]

We next investigated the influence of elevated temperature on the coverage and structure of adsorbed insulin by heating the solution and ATR crystal to 65 °C. To this end, we prepared insulin layers on ATR crystals ex situ and recorded spectra of dried insulin layers, which shifts the amide I maximum by 7 cm^{-1} due to removal of the hydration layer. Having established from FTIR spectra of the wet layers shown in Figure 3 that the structure of adsorbed insulin is nearly native, we can use dried layers as a reference for adsorbed insulin with native secondary structure but without its hydration shell. In order to stabilize the physisorbed insulin layer on the hydrophilic surface for ATR analysis, we rinsed directly with water rather than buffer after immersion in insulin solution. The sudden change back to neutral pH means a reduction in the repulsion between HI and APTMS and therefore a higher residual coverage. This is also supported by QCM-D results using water rinsing immediately after the insulin adsorption phase, resulting in significantly thicker residual protein layers (data not shown). The good agreement in the coverages obtained for ex situ and in situ ATR measurements on APTMS seen in Figure 4 shows the success of this strategy. Rinsing the crystal, however, does not always remove all traces of citrate ions, so in our discussion, we ignore the changes in the citrate peak found between 1700 and 1750 cm^{-1} for dry layers.

The maximum adsorption time was limited to 20 h by gradual D/H exchange with water vapor in the air. Figure 4 shows that extending the adsorption time on the hydrophobic TMPS-terminated surface at room temperature from 1 to 20 h hardly changes the peak shape at all. This hydrophobic surface is therefore insulin-friendly for an extended time under acidic conditions at room temperature. The coverage after 20 h of incubation in room-temperature solution is close to 4 mg/m^2, i.e., a low multilayer coverage of insulin. The same coverage can be reached after 4 h of incubation at 65 °C, but now with a clear β-sheet spectral signature at 1624 cm^{-1}. As the scaled spectra in Figure 4 show, the overall shape of the amide I band changes only marginally during subsequent growth. It should be noted that while the relative β-sheet content decreases from around 6% for 4 h of incubation to 3% for 20 h of incubation, the absolute amount of the β-sheet still increases, since the coverage increases 10-fold over this time range.

The hydrophilic APTMS-terminated surface stabilizes the adsorbed insulin conformation for at least 8 h at 65 °C, and a minor β-sheet-related shoulder at ∼1630 cm^{-1} appears only after heating for 20 h. This supports the literature finding that insulin bound to APTMS-covered silica beads is still physiologically active.[21]

DOI: 10.1021/acs.langmuir.5b01477
Langmuir 2015, 31, 8892−8900

DISCUSSION

The data presented in this work demonstrate that insulin monomers maintain their native secondary structure when adsorbed on both hydrophobic and hydrophilic surfaces at low pH at room temperature. This is in marked contrast to detailed structural studies at physiological pH, which find evidence of changes in secondary structural content.[10,15] We propose that the known acid stabilization of human insulin and the protection of the aggregation-prone hydrophobic domains on the insulin monomer by adsorption on the hydrophobic surface work together to inhibit fibril formation at room temperature.

Fibrillation is generally described as a nucleation-induced event, where misfolded proteins assemble into a small oligomeric nucleus, which then elongates into a fibril. The accelerating effect of surfaces is accordingly ascribed to a local enhancement of the protein concentration through adsorption and/or to the stabilization of misfolded, adsorbed proteins. For example, recent studies of the surface-induced fibrillation of α-synuclein and amyloid-β showed that nanomolar concentrations are sufficient, whereas fibrillation in the bulk requires micromolar solutions.[50,51] In the case of amyloid-β, the on-surface diffusion rate was revealed as a critical parameter; no fibrils formed if the peptide was too strongly adsorbed, whereas intermediate binding resulted in sufficient mobility to promote interactions between peptides, which led to fibril formation.[51]

A surface-induced change in the conformation of the adsorbed peptide is also a frequently considered factor, in particular on hydrophobic surfaces. Adsorption is driven by the dehydration of hydrophobic side chains, but adsorbed peptides can compensate for the accompanying loss of hydrogen bonds by forming new hydrogen bonds with neighboring peptides which then leads to β-sheet formation within the surface plane.[52] A structural change in adsorbed insulin, for example, was concluded from binding of the bacterial chaperone DnaK to adsorbed insulin.[53] DnaK can bind only to amyloidogenic insulin fragment LVEALYL, which is protected from the solution inside the B-chain helix in native insulin. Preadsorbed β-sheets were indeed shown to act as an efficient nucleus and accelerant for insulin fibrillation.[16]

While there is plenty of evidence to show that hydrophobic surfaces accelerate insulin fibrillation, only very few spectroscopic studies have determined the actual structure of adsorbed insulin at the single layer or low multilayer level. Jorgensen et al. studied UV circular dichroism spectra of a variety of insulin variants on Teflon beads at pH 7.4 and generally reported a decrease in α-helical content and an increase in random coils.[10] Nault et al. used ATR-FTIR to observe the amide I band of thin layers of insulin adsorbed at pD 6.9 on a diphenyl-functionalized silicon ATR crystal.[15] They report the appearance of a peak at 1708 cm^{-1} which was assigned to an intermolecular β-sheet, although the normally dominant β-sheet vibration at around 1630 cm^{-1} was entirely absent.

Our amide I spectra show on the contrary that no structural changes occur in adsorbed insulin in the 1−4 mg/m^2 coverage regime over extended incubation times at room temperature. The main difference with respect to prior studies is incubation in acidic insulin solutions. Acidic solutions generally aid fibril formation in the bulk because the low pH increases the fraction of aggregation-prone insulin monomers in the solution. However, acidic pH also increases the Gibbs free energy of unfolding of biosynthetic human insulin by 30% due to an additional hydrogen bond between His-B5 and one of the main-chain carbonyl oxygens of Cys-A7 or Ser-A9.[54] This helps to maintain the structure by connecting the N-terminal region of the B chain to the A-chain loop between the two helices.

The driving force for insulin monomer adsorption to hydrophobic surfaces is the entropy gain from water repulsion and is similar to the hydrophobic interaction to form the dimer, although the latter is made more specific by hydrogen-bond formation.[11] This hydrophobic interaction causes a segregation of the monomer to the hydrophobic air/water interface regardless of bulk oligomer composition, as demonstrated recently by SFS.[29] The hydrophobic forces are strong enough to overcome the repulsion between the highly charged insulin monomers in a low-ionic-strength solution, as shown for the adsorption of various modified insulin variants on polystyrene and Teflon beads.[10,14]

Nilsson et al. were the first to propose that the residues involved in the dimer interface bind to hydrophobic surfaces. These are mostly found in the extended chain from residues B23 to B28.[18] Mollmann et al.[13] later confirmed this model through a shift in the tryptophan fluorescence wavelength of Trp^{B30}-modified insulin. Such binding of the dimer interface to the hydrophobic surface could maintain the overall structure of insulin in its native, globular shape. It would also produce a net orientation of side chains, which is compatible with the finding from SFS (vide supra). This net monomer orientation then exposes the more hydrophilic side chains to the solvent, as evidenced by the increased hydrophilicity of the surface after insulin adsorption. Adsorption of the first layer of insulin therefore changes the character of the solvent-accessible surface from hydrophobic to hydrophilic, which effectively slows down further adsorption.

On the hydrophilic surface, insulin forms a mainly physisorbed layer, as the difference between the net QCM-D response and the in situ infrared absorbance shows. This leads to a more random orientation of adsorbed insulin, thus explaining why there is no net contribution from insulin side chains evident in the sum frequency spectra. At higher temperatures, binding between positively charged $-NH_3^+$ and negatively charged side chains becomes possible. In the reaction between $-NH_3^+$ terminated Si(100) and glycine, Kim et al. found that the carboxyl group of glycine can react with the amine group on heating to above 50 °C.[55] The C termini of the A and B chains (Asp and Thr, respectively) of insulin could electrostatically attach to or react with the $-NH_3^+$-terminated surface, with the A chain being the more likely candidate, as most of the positive charges are found within the insulin B chain. It is conceivable that this localized attraction already plays a role at room temperature, which would explain why the APTMS chains reorient, as shown by the change in the SF spectrum of their residual methoxy groups.

Even though the hydrophobic interaction stabilizes the insulin native state for extended times on the hydrophobic surface, heating to 65 °C is sufficient to cause restructuring of the adsorbed insulin layer. After 4 h of incubation under heat, the amide I band signals a structural change from native to a distinct β-sheet with a signature band at 1625 cm^{-1}, at a coverage that corresponds to at most four layers of insulin (3.8 mg/m^2), close to the 3.9 mg/m^2 achieved after 20 h of incubation in a room-temperature solution. The change in structure is clearly identifiable but does not represent a fully formed insulin fibril yet, since solution-formed insulin fibrils are characterized by an amide I band with about 70% of the area contained in the β-sheet at 1630 cm^{-1} (Supporting

DOI: 10.1021/acs.langmuir.5b01477
Langmuir 2015, 31, 8892−8900

Information), while the amide I band after 4 h of incubation contains only approximately 6% β-sheet.

After the layer has thus been restructured, the insulin coverage rapidly increases compared to cold incubation and after 20 h reaches 39 mg/m^2. This conforms to the previously discussed model of a conformation change at the surface leading to accelerated aggregation. The amide I band shape of the initially restructured layer is preserved to a very large degree as seen in Figure 4. The intermediate on the path to fibril formation can thus be clearly identified as a partially denatured insulin layer, which provides the template for further growth.

On the hydrophilic surface, a slight broadening occurs after 8 h of incubation under heat, and only after 20 h can we diagnose a very small presence of β-sheet structure at a coverage of 2.6 mg/m^2. The surface coverage over this time range remains well below the coverage on the hydrophobic surface, leading us to speculate that the critical nucleus size is close to a coverage of 4 mg/m^2.

While the hydrophobic interaction of insulin with the methyl-terminated hydrophobic surface used here was not sufficient to stabilize the adsorbed protein under heat, it is possible that a better designed surface with additional aromatic or H-bonding species could provide additional interactions with the protein to better mimic the hydrophobic dimer interface and stabilize adsorbed insulin to the same degree as in bulk solution. Therefore, the inhibition of adsorption is not the only option available for preventing fibril formation; the stabilization of an adsorbed native state is also a conceivable prospect.

CONCLUSIONS

Our measurements demonstrate that the adsorption of insulin at acidic pH on solid, hydrophobic surfaces can lead to a nearly native secondary structure of the protein, which is stable at room temperature. Hydrophobic surfaces are therefore not detrimental to the native structure of insulin per se, as they can shield the aggregation-prone hydrophobic domains on the insulin monomer from other monomers in solution. Indeed, we discovered that significant thermal activation is needed before restructuring occurs. The observation of insulin secondary structure under heat showed in addition that a restructured adsorbed insulin layer should be considered to be the intermediate species on the way to fibrillation.

ASSOCIATED CONTENT

Supporting Information

The Supporting Information is available free of charge on the ACS Publications website at DOI: 10.1021/acs.langmuir.5b01477.

X-ray photoelectron spectroscopy. Quartz crystal microbalance with dissipation. Quantification by attenuated total internal reflection infrared spectroscopy. Sum frequency spectral analysis. (PDF)

AUTHOR INFORMATION

Corresponding Author

*E-mail: Heike.Arnolds@liv.ac.uk.

Author Contributions

The manuscript was written through the contributions of all authors. All authors have given approval to the final version of the manuscript.

Notes

The authors declare no competing financial interest.

ACKNOWLEDGMENTS

S.M. gratefully acknowledges Sanofi-Aventis Deutschland GmbH (Frankfurt) for a studentship. We thank Benjamin Johnson (Leeds University) for his help with QCM and XPS and his advice on surface preparation, Prof. Evans and the Molecular and Nanoscale Physics Group at Leeds University in general for their hospitality, Caroline Smith (University of Liverpool) and Usha Devi (Biolin Scientific) for further help with QCM-D, and the Photon Science Institute in Manchester for access to their sum frequency spectrometer.

REFERENCES

(1) Cherny, I.; Gazit, E.; Amyloids. Not Only Pathological Agents but Also Ordered Nanomaterials. *Angew. Chem., Int. Ed.* **2008**, *47* (22), 4062−4069.

(2) Sipe, J. D.; Cohen, A. S. Review: History of the Amyloid Fibril. *J. Struct. Biol.* **2000**, *130* (2−3), 88−98.

(3) Jiménez, J. L.; Nettleton, E. J.; Bouchard, M.; Robinson, C. V.; Dobson, C. M.; Saibil, H. R. The protofilament structure of insulin amyloid fibrils. *Proc. Natl. Acad. Sci. U. S. A.* **2002**, *99* (14), 9196−9201.

(4) Arora, A.; Ha, C.; Park, C. B. Inhibition of insulin amyloid formation by small stress molecules. *FEBS Lett.* **2004**, *564* (1−2), 121−125.

(5) Hong, Y.; Meng, L.; Chen, S.; Leung, C. W. T.; Da, L.-T.; Faisal, M.; Silva, D.-A.; Liu, J.; Lam, J. W. Y.; Huang, X.; Tang, B. Z. Monitoring and Inhibition of Insulin Fibrillation by a Small Organic Fluorogen with Aggregation-Induced Emission Characteristics. *J. Am. Chem. Soc.* **2012**, *134* (3), 1680−1689.

(6) Hua, Q. X.; Weiss, M. A. Mechanism of insulin fibrillation: the structure of insulin under amyloidogenic conditions resembles a protein-folding intermediate. *J. Biol. Chem.* **2004**, *279* (20), 21449−60.

(7) Whittingham, J. L.; Scott, D. J.; Chance, K.; Wilson, A.; Finch, J.; Brange, J.; Guy Dodson, G. Insulin at pH 2: Structural Analysis of the Conditions Promoting Insulin Fibre Formation. *J. Mol. Biol.* **2002**, *318* (2), 479−490.

(8) Sharp, J. S.; Forrest, J. A.; Jones, R. A. L. Surface denaturation and amyloid fibril formation of insulin at model lipid-water interfaces. *Biochemistry* **2002**, *41* (52), 15810−15819.

(9) Smith, M. I.; Sharp, J. S.; Roberts, C. J. Nucleation and growth of insulin fibrils in bulk solution and at hydrophobic polystyrene surfaces. *Biophys. J.* **2007**, *93* (6), 2143−2151.

(10) Jorgensen, L.; Bennedsen, P.; Hoffmann, S. V.; Krogh, R. L.; Pinholt, C.; Groenning, M.; Hostrup, S.; Bukrinsky, J. T. Adsorption of insulin with varying self-association profiles to a solid Teflon surface-Influence on protein structure, fibrillation tendency and thermal stability. *Eur. J. Pharm. Sci.* **2011**, *42* (5), 509−516.

(11) Nilsson, P.; Nylander, T.; Havelund, S. Adsorption of Insulin on Solid-Surfaces in Relation to the Surface-Properties of the Monomeric and Oligomeric Forms. *J. Colloid Interface Sci.* **1991**, *144* (1), 145−152.

(12) Mollmann, S. H.; Bukrinsky, J. T.; Frokjaer, S.; Elofsson, U. Adsorption of human insulin and AspB28 insulin on a PTFE-like surface. *J. Colloid Interface Sci.* **2005**, *286* (1), 28−35.

(13) Mollmann, S. H.; Jorgensen, L.; Bukrinsky, J. T.; Elofsson, U.; Norde, W.; Frokjaer, S. Interfacial adsorption of insulin: Conformational changes and reversibility of adsorption. *Eur. J. Pharm. Sci.* **2006**, *27* (2−3), 194−204.

(14) Pinholt, C.; Hostrup, S.; Bukrinsky, J. T.; Frokjaer, S.; Jorgensen, L. Influence of Acylation on the Adsorption of Insulin to Hydrophobic Surfaces. *Pharm. Res.* **2011**, *28* (5), 1031−1040.

(15) Nault, L.; Guo, P.; Jain, B.; Brechet, Y.; Bruckert, F.; Weidenhaupt, M. Human insulin adsorption kinetics, conformational changes and amyloidal aggregate formation on hydrophobic surfaces. *Acta Biomater.* **2013**, *9* (2), 5070−9.

(16) Nault, L.; Vendrely, C.; Bréchet, Y.; Bruckert, F.; Weidenhaupt, M. Peptides that form β-sheets on hydrophobic surfaces accelerate

DOI: 10.1021/acs.langmuir.5b01477
Langmuir 2015, 31, 8892−8900

surface-induced insulin amyloidal aggregation. *FEBS Lett.* **2013**, *587* (9), 1281−1286.
(17) Bocian, W.; Kozerski, L. 2JV1: NMR Structure of Human Insulin Monomer in 35% CD3CN Zinc Free, 50 Structures. *Worldwide Protein Data Bank*, 2007.
(18) Baker, E. N.; Blundell, T. L.; Cutfield, J. F.; Cutfield, S. M.; Dodson, E. J.; Dodson, G. G.; Hodgkin, D. M. C.; Hubbard, R. E.; Isaacs, N. W.; Reynolds, C. D.; Sakabe, K.; Sakabe, N.; Vijayan, N. M. *Philos. Trans. R. Soc., B* **1988**, *319*, 369−456.
(19) Humphrey, W.; Dalke, A.; Schulten, K. VMD: Visual molecular dynamics. *J. Mol. Graphics* **1996**, *14* (1), 33−38.
(20) Reichhart, C.; Czeslik, C. Native-like Structure of Proteins at a Planar Poly(acrylic acid) Brush. *Langmuir* **2009**, *25* (2), 1047−1053.
(21) Mansur, H. S.; Oréfice, R. L.; Vasconcelos, W. L.; Lobato, Z. P.; Machado, L. J. C. Biomaterial with chemically engineered surface for protein immobilization. *J. Mater. Sci.: Mater. Med.* **2005**, *16* (4), 333−340.
(22) Kim, J.; Holinga, G. J.; Somorjai, G. A. Curing Induced Structural Reorganization and Enhanced Reactivity of Amino-Terminated Organic Thin Films on Solid Substrates: Observations of Two Types of Chemically and Structurally Unique Amino Groups on the Surface. *Langmuir* **2011**, *27* (9), 5171−5175.
(23) Arnebrant, T.; Nylander, T. Adsorption of insulin on metal surfaces in relation to association behavior. *J. Colloid Interface Sci.* **1988**, *122* (2), 557−566.
(24) Lau, W. M.; Bello, I.; Huang, L. J.; Feng, X.; Vos, M.; Mitchell, I. V. Argon incorporation in Si(100) by ion bombardment at 15−100 eV. *J. Appl. Phys.* **1993**, *74* (12), 7101−7106.
(25) Dzwolak, W.; Ravindra, R.; Winter, R. Hydration and structure-the two sides of the insulin aggregation process. *Phys. Chem. Chem. Phys.* **2004**, *6* (8), 1938−1943.
(26) Guo, Z.; Zheng, W.; Hamoudi, H.; Dablemont, C.; Esaulov, V. A.; Bourguignon, B. On the chain length dependence of CH3 vibrational mode relative intensities in sum frequency generation spectra of self assembled alkanethiols. *Surf. Sci.* **2008**, *602* (23), 3551−3559.
(27) Attri, A. K.; Fernández, C.; Minton, A. P. pH-dependent self-association of zinc-free insulin characterized by concentration-gradient static light scattering. *Biophys. Chem.* **2010**, *148* (1−3), 28−33.
(28) Xu, Y.; Yan, Y.; Seeman, D.; Sun, L.; Dubin, P. L. Multimerization and Aggregation of Native-State Insulin: Effect of Zinc. *Langmuir* **2012**, *28* (1), 579−586.
(29) Mauri, S.; Weidner, T.; Arnolds, H. The structure of insulin at the air/water interface: monomers or dimers? *Phys. Chem. Chem. Phys.* **2014**, *16* (48), 26722−26724.
(30) Pohl, R.; Hauser, R.; Li, M.; De Souza, E.; Feldstein, R.; Seibert, R.; Ozhan, K.; Kashyap, N.; Steiner, S. Ultra-Rapid Absorption of Recombinant Human Insulin Induced by Zinc Chelation and Surface Charge Masking. *J. Diabetes Sci. Technol.* **2012**, *6* (4), 755−763.
(31) Brange, J. *Galenics of Insulin*; Springer: 1987.
(32) Ray, S.; Shard, A. G. Quantitative Analysis of Adsorbed Proteins by X-ray Photoelectron Spectroscopy. *Anal. Chem.* **2011**, *83* (22), 8659−8666.
(33) Evers, F.; Reichhart, C.; Steitz, R.; Tolan, M.; Czeslik, C. Probing adsorption and aggregation of insulin at a poly(acrylic acid) brush. *Phys. Chem. Chem. Phys.* **2010**, *12* (17), 4375−82.
(34) Quast, A. D.; Wilde, N. C.; Matthews, S. S.; Maughan, S. T.; Castle, S. L.; Patterson, J. E. Improved assignment of vibrational modes in sum-frequency spectra in the CH stretch region for surface-bound C18 alkylsilanes. *Vib. Spectrosc.* **2012**, *61*, 17−24.
(35) Liu, Y.; Wolf, L. K.; Messmer, M. C. A Study of Alkyl Chain Conformational Changes in Self-Assembled n-Octadecyltrichlorosilane Monolayers on Fused Silica Surfaces. *Langmuir* **2001**, *17*, 4329−4335.
(36) Bourguignon, B.; Zheng, W.; Carrez, S.; Ouvrard, A.; Fournier, F.; Dubost, H. Deriving the complete molecular conformation of self-assembled alkanethiol molecules from sum-frequency generation vibrational spectra. *Phys. Rev. B: Condens. Matter Mater. Phys.* **2009**, *79*, 12.
(37) Hirose, C.; Akamatsu, N.; Domen, K. Formulas for the analysis of surface sum-frequency generation spectrum by CH stretching modes of methyl and methylene groups. *J. Chem. Phys.* **1992**, *96* (2), 997−1004.
(38) Shaw, S. K.; Lagutchev, A.; Dlott, D. D.; Gewirth, A. A. Electrochemically Driven Reorientation of Three Ionic States of p-Aminobenzoic Acid on Ag(111). *J. Phys. Chem. C* **2009**, *113* (6), 2417−2424.
(39) Mengistu, T. Z.; Goel, V.; Horton, J. H.; Morin, S. Chemical force titrations of functionalized Si(111) surfaces. *Langmuir* **2006**, *22* (12), 5301−5307.
(40) Allen, G. C.; Sorbello, F.; Altavilla, C.; Castorina, A.; Ciliberto, E. Macro-, micro- and nano-investigations on 3-aminopropyltrimethoxysilane self-assembly-monolayers. *Thin Solid Films* **2005**, *483* (1−2), 306−311.
(41) Wang, H.-F.; Gan, W.; Lu, R.; Rao, Y.; Wu, B.-H. Quantitative spectral and orientational analysis in surface sum frequency generation vibrational spectroscopy (SFG-VS). *Int. Rev. Phys. Chem.* **2005**, *24* (2), 191−256.
(42) Gough, K. M. Theoretical analysis of molecular polarizabilities and polarizability derivatives in hydrocarbons. *J. Chem. Phys.* **1989**, *91* (4), 2424−2432.
(43) Wei, X.; Hong, S.-C.; Zhuang, X.; Goto, T.; Shen, Y. R. Nonlinear optical studies of liquid crystal alignment on a rubbed polyvinyl alcohol surface. *Phys. Rev. E: Stat. Phys., Plasmas, Fluids, Relat. Interdiscip. Top.* **2000**, *62* (4), 5160−5172.
(44) Weber, J.; Balgar, T.; Hasselbrink, E. Conformational disorder in alkylsiloxane monolayers at elevated temperatures. *J. Chem. Phys.* **2013**, *139* (24), 244902.
(45) Holinga, G. J.; York, R. L.; Onorato, R. M.; Thompson, C. M.; Webb, N. E.; Yoon, A. P.; Somorjai, G. A. An SFG study of interfacial amino acids at the hydrophilic SiO2 and hydrophobic deuterated polystyrene surfaces. *J. Am. Chem. Soc.* **2011**, *133* (16), 6243−53.
(46) Wang, J.; Chen, X.; Clarke, M. L.; Chen, Z. Vibrational spectroscopic studies on fibrinogen adsorption at polystyrene/protein solution interfaces: hydrophobic side chain and secondary structure changes. *J. Phys. Chem. B* **2006**, *110* (10), 5017−24.
(47) Phillips, D. C.; York, R. L.; Mermut, O.; McCrea, K. R.; Ward, R. S.; Somorjai, G. A. Side chain, chain length, and sequence effects on amphiphilic peptide adsorption at hydrophobic and hydrophilic surfaces studied by sum-frequency generation vibrational spectroscopy and quartz crystal microbalance. *J. Phys. Chem. C* **2007**, *111* (1), 255−261.
(48) Bulard, E.; Guo, Z.; Zheng, W.; Dubost, H.; Fontaine-Aupart, M. P.; Bellon-Fontaine, M. N.; Herry, J. M.; Briandet, R.; Bourguignon, B. Non-invasive vibrational SFG spectroscopy reveals that bacterial adhesion can alter the conformation of grafted ″brush″ chains on SAM. *Langmuir* **2011**, *27* (8), 4928−35.
(49) Goormaghtigh, E.; Cabiaux, V.; Ruysschaert, J.-M. Determination of Soluble and Membrane Protein Structure by Fourier Transform Infrared Spectroscopy. In *Physicochemical Methods in the Study of Biomembranes*; Hilderson, H., Ralston, G., Eds.; Plenum Press: New York, 1994; Vol. *23*, pp 329−362.
(50) Rabe, M.; Soragni, A.; Reynolds, N. P.; Verdes, D.; Liverani, E.; Riek, R.; Seeger, S. On-Surface Aggregation of alpha-Synuclein at Nanomolar Concentrations Results in Two Distinct Growth Mechanisms. *ACS Chem. Neurosci.* **2013**, *4* (3), 408−417.
(51) Shen, L.; Adachi, T.; Vanden Bout, D.; Zhu, X. Y. A Mobile Precursor Determines Amyloid-β Peptide Fibril Formation at Interfaces. *J. Am. Chem. Soc.* **2012**, *134* (34), 14172−14178.
(52) Nikolic, A.; Baud, S.; Rauscher, S.; Pomes, R. Molecular mechanism of beta-sheet self-organization at water-hydrophobic interfaces. *Proteins: Struct., Funct., Genet.* **2011**, *79* (1), 1−22.
(53) Ballet, T.; Brukert, F.; Mangiagalli, P.; Bureau, C.; Boulange, L.; Nault, L.; Perret, T.; Weidenhaupt, M. DnaK prevents human insulin amyloid fiber formation on hydrophobic surfaces. *Biochemistry* **2012**, *51* (11), 2172−80.

DOI: 10.1021/acs.langmuir.5b01477
Langmuir 2015, 31, 8892−8900

(54) Bryant, C.; Spencer, D. B.; Miller, A.; Bakaysa, D. L.; McCune, K. S.; Maple, S. R.; Pekar, A. H.; Brems, D. N. Acid Stabilization of Insulin. *Biochemistry* **1993**, *32* (32), 8075−8082.
(55) Kim, M. K.; Baik, J.; Jeon, C.; Song, I.; Nam, J. H.; Hwang, H. N.; Hwang, C. C.; Woo, S. H.; Park, C. Y.; Ahn, J. R. Biological functionalization of the amine-terminated Si(100) surface by glycine. *Surf. Sci.* **2010**, *604* (19−20), 1598−1602.

DOI: 10.1021/acs.langmuir.5b01477
Langmuir 2015, 31, 8892−8900